

Local lattice instability and stripes in the CuO_2 plane of the $\text{La}_{1.85}\text{Sr}_{0.15}\text{CuO}_4$ system by polarized XANES and EXAFS

N. L. Saini and A. Lanzara

Dipartimento di Fisica and Istituto Nazionale di Fisica Nucleare (INFN), Università di Roma "La Sapienza," P. A. Moro 2, 00185 Roma, Italy

H. Oyanagi, H. Yamaguchi, K. Oka, and T. Ito

Electrotechnical Laboratory, Umezono, Tsukuba, Ibaraki 305, Japan

A. Bianconi

Dipartimento di Fisica, Università di Roma "La Sapienza," P. A. Moro 2, 00185 Roma, Italy

(Received 8 May 1996; revised manuscript received 5 November 1996)

Temperature-dependent polarized Cu K -edge x-ray absorption has been used to investigate local structural distortions in the CuO_2 plane of the $\text{La}_{1.85}\text{Sr}_{0.15}\text{CuO}_4$ system. The Cu-O pair distribution shows the presence of a minority phase containing CuO_6 octahedra characterized by a shorter Cu-O(apical) bond ($\Delta R \sim -0.1 \text{ \AA}$) and two longer Cu-O(planar) bonds ($\Delta R \sim +0.08 \text{ \AA}$) and a tilting angle of $16^\circ \pm 2^\circ$. The temperature-dependent distortions show a maximum around T^* ($\sim 1.6T_c$) and a minimum at T_c ($\sim 35 \text{ K}$). The data show the coexistence of two types of doped charges in different stripes in the superconducting phase. [S0163-1829(97)03214-1]

I. INTRODUCTION

Experimental methods which probe local structure have shown that the local structure of the CuO_2 plane is different from the average structure in most of the superconducting cuprate perovskites.¹⁻³⁶ Steric effects due to dopants in the rocksalt layers, lattice distortions associated with the doped holes in the CuO_2 plane, or lattice mismatch³⁴ could all be the origin of the divergence of the local structure from the average one.

Cu K -edge x-ray absorption spectroscopy [x-ray absorption near edge structure (XANES) and extended x-ray absorption fine structure (EXAFS)] has been exploited to investigate the local structure near a selected atomic site.³⁷ XANES and EXAFS are a type of electron diffraction in which the central atom plays the role of both source and detector for photoelectrons backscattered by neighboring atoms. Cu K -edge absorption spectra of high- T_c systems³⁸⁻⁴⁰ probe the geometry of a local cluster of about 50 atoms within a radius of 5 \AA from the central Cu. EXAFS data analysis³⁹⁻⁴⁰ provides the pair correlation function and XANES probes the higher order correlation function within the cluster of atoms. Polarized spectra provide a unique possibility to separate the contributions of the in-plane and out-of-plane backscattering and have been used to determine the Cu-O(planar) and Cu-O(apical) bond lengths by independent measurements. This approach has given experimental evidence for the stripe structure of the CuO_2 plane in $\text{Bi}_2\text{Sr}_2\text{CaCu}_2\text{O}_{8+y}$ (Bi2212) system.¹¹⁻¹⁴

$\text{La}_{1.85}\text{Sr}_{0.15}\text{CuO}_4$ (LSCO) can be considered the simplest superconducting system at the optimum doping for determining the characteristic properties of the metallic CuO_2 plane in high- T_c cuprates. The average structure of the system shows a macroscopic phase transition from a high-temperature tetragonal (HTT) to a low-temperature orthorhombic (LTO)

structure at about 200 K .^{29,41,42} Below the $\text{HTT} \rightarrow \text{LTO}$ transition the system undergoes a broad crossover in the electronic, magnetic, and structural properties. The coexistence of local domains with a lattice similar to a low-temperature tetragonal (LTT) phase¹⁶ within the LTO phase has been found.¹⁵ The presence of different Cu sites in the isostructural, oxygen doped, La_2CuO_4 characterized by different tilting angles θ of the CuO_6 octahedra with ($0^\circ < \theta < 18^\circ$), has been shown by nuclear magnetic resonance (NMR) spectroscopy.⁴ Temperature dependent anomalies at T_c , seen in inelastic neutron scattering³¹ and pair distribution function (PDF) analysis of powder neutron diffraction data,² have been interpreted as evidence of divergence of the local structure of the system from the average one. The anomalous behavior of the elastic constant at about 60 K (Ref. 25) has been interpreted as evidence for a frustrated phase transition at this temperature with formation of LTT domains.

The divergence of the local structure from the average one has also been indicated by EXAFS experiment⁴⁰ made in the early days of high- T_c superconductivity research. The average Cu-O(apical) bond length was found to be 2.32 \AA instead of 2.4 \AA reported by diffraction. The polarized Cu K -edge EXAFS reported in the present paper is aimed at characterizing the minority phase in the average crystallographic structure of the LSCO by determining directly the Cu-O bond lengths. Part of this work has been published in a recent letter.⁴³ The ability of EXAFS to solve the different local bond lengths was well demonstrated in solid solutions⁴⁴ while the diffraction data provided only the average distance. In the present experiment, the Cu-O(planar) bond lengths have been measured with $\mathbf{E} \parallel \mathbf{ab}$ and the Cu-O(apical) bond lengths with $\mathbf{E} \parallel \mathbf{c}$. Critical for the success of the experiment was the use of a high quality single crystal and EXAFS data with high signal-to-noise ratio. The temperature dependence of the bond distances was measured systematically in order

to identify the onset of the local lattice distortions and their correlation with the structural anomalies. From joint analysis of EXAFS data and diffuse x-ray scattering the stripe structure of the CuO₂ plane was determined.

The experiment and the data analysis procedure are described in Sec. II. Experimental results are reported in Sec. III. The temperature dependence of the raw XANES data and of the EXAFS Fourier transforms provide clear evidence for anomalous changes in the local geometry at two characteristic temperatures: the superconducting transition temperature T_c , and a temperature $T^* \sim 1.6T_c$. Local distortions in the CuO₂ plane are determined from the analysis of the Cu-O(planar) and Cu-O(apical) EXAFS signals show the coexistence of two different structural conformations of the CuO₆ octahedra below 100 K, characterized by two different Cu-O(planar) bonds ($\Delta R = +0.08$ Å), and a tilting angle $\theta = 16^\circ \pm 2^\circ$. We compare the present findings with diffraction results in the final part of Sec. III. The results are discussed in Sec. IV and the stripe structure of the CuO₂ plane is presented. Section V provides summary and conclusions.

II. EXPERIMENT AND DATA ANALYSIS

Measurements were made on a well-characterized single crystal, $3 \times 2 \times 0.5$ mm³, grown by the traveling solvent floating zone method, showing a sharp superconducting transition at $T_c = 35$ K. Temperature dependent polarized Cu *K*-edge absorption measurements were performed on beam-line BL-4C (Ref. 45) at the Photon Factory at Tsukuba. The synchrotron radiation emitted by the 2.5 GeV storage ring at a typical current of 350 mA was monochromatized by a fixed-exit double crystal Si(111) monochromator (giving a resolution of ~ 1.6 eV at the Cu *K* edge) and sagittally focused on the sample. The spectra were recorded by detecting the fluorescence yield (FY) using 9 NaI(Tl) x-ray detectors covering a large solid angle of the x-ray fluorescence emission. The sample was mounted in a closed-cycle He refrigerator and the temperature was monitored with an accuracy of ± 0.5 K. The drift in the energy calibration, estimated by calibrations before and after the experiment, was below 5% of the energy resolution. In order to minimize drift, the monochromator crystal was kept irradiated throughout the experiment and the Bragg angle was monitored by a directly coupled encoder with an accuracy of 1 arcsec.

The $\mathbf{E} \parallel \mathbf{ab}$ absorption spectra were recorded by keeping the sample at the normal incidence while the $\mathbf{E} \parallel \mathbf{c}$ spectra were collected by keeping the sample near the grazing incidence (10°). The true $\mathbf{E} \parallel \mathbf{c}$ spectra have been obtained by extrapolation of the spectra recorded at the grazing incidence and using the $\mathbf{E} \parallel \mathbf{ab}$ signal. The EXAFS signal $\chi = (\alpha - \alpha_0)/\alpha_0$ (where α is the absorption coefficient and α_0 is the so called atomic absorption) was extracted from the absorption spectrum using standard procedure³⁷ and corrected for fluorescence self-absorption.⁴⁶

The EXAFS signal depends on several parameters, as can be seen from the following equation for polarized *K*-edge EXAFS:

$$\chi(k) = \frac{m\pi}{h^2} \sum_i 3N_i \cos^2(\theta_i) \frac{S_0^2}{kR_i^2} f_i(k, R_i) e^{-2R_i/\lambda} e^{-2k^2\sigma_i^2} \times \sin[2kR_i + \delta_i(k)],$$

where N_i is the equivalent number of neighboring atoms at a distance R_i located at angle (θ_i) with respect to the electric field vector of the polarized synchrotron light.³⁷ S_0^2 is an amplitude correction factor due to photoelectron correlations and is also called passive electrons reduction factor, $f_i(k, R_i)$ is the backscattering amplitude, λ is the photoelectron mean free path, and σ^2 is the correlated Debye-Waller factor of the photoabsorber-backscatterer pairs. Apart from the above, the photoelectron energy origin E_0 and the phase shifts δ_i should be known. The above parameters can be either fixed or allowed to vary when an experimental EXAFS spectrum is parameterized.

The phase shifts were calculated using the EXCURVE92 (Ref. 47) and FEFF6 (Ref. 48) codes and were found to agree with each other for the Cu-O pair in the present system. The fitting procedure is based on a standard nonlinear least squares technique which minimizes the statistical χ^2 determined by the squares of the difference between the experimental and theoretical EXAFS. The number of independent parameters which may be determined by EXAFS are limited by the number of independent data points, $N_{\text{ind}} \sim (2\Delta k \Delta R)/\pi$, where Δk and ΔR are respectively the ranges in k and R space over which the data are fitted.³⁷ N_{ind} is ≈ 7 ($\Delta k = 16 - 3 = 13$ Å⁻¹ and $\Delta R = 0.8$ Å) for the analysis of the Cu-O shell.

Reported errors in the parameters were estimated by the standard EXAFS (parabola) method⁴⁹⁻⁵¹ in which the quality of fit parameter (proportional to the statistical χ^2) is plotted as a function of the concerned parameter. Errors are usually estimated from a fractional increase δ of χ^2 above its minimum value. This fraction δ depends on several experimental and data analysis factors. In order to establish the reported uncertainties we have analyzed four independent EXAFS scans at each temperature. Parameters and errors were checked by analyzing the data using different recent versions of EXAFS data analysis codes including EXCURVE,⁴⁷ NPI,⁵² and EDA (Exafs Data Analysis) (Ref. 53) and the results obtained fall within the quoted uncertainties.

III. RESULTS

A. Anomalous behavior of the local geometry: The XANES results

Figure 1 shows normalized Cu *K*-edge XANES spectra measured at low temperature (21 K) with \mathbf{E} parallel [$\mathbf{E} \parallel \mathbf{ab}$, panel (a)] and normal [$\mathbf{E} \parallel \mathbf{c}$, panel (b)] to the *ab* plane of the LSCO crystal. The derivative spectrum and a typical absorption difference with respect to the 21 K are also included in the two panels. The spectra show the usual characteristic features observed in Cu *K*-edge XANES of the cuprates with square planar geometry. We have denoted the well-resolved features (absorption maxima) by A_1, A_2, A_3 in the $\mathbf{E} \parallel \mathbf{c}$ spectrum and B_0, B_1, B_2 in the $\mathbf{E} \parallel \mathbf{ab}$ spectrum. The energy positions $\alpha_1, \alpha_2, \alpha_3$ and $\beta_0, \beta_1, \beta_2$, respectively correspond to the rising edges of the features as determined by the derivative spectrum.

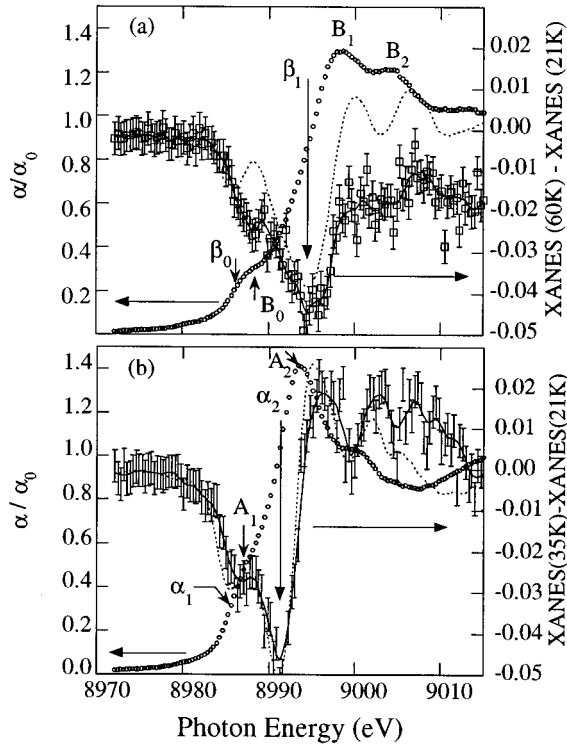


FIG. 1. Polarized Cu K -edge XANES spectra of single crystal $\text{La}_{1.85}\text{Sr}_{0.15}\text{CuO}_4$ in (a) $\mathbf{E}\parallel\mathbf{ab}$ geometry at 21 K, derivative spectrum times -1 (dotted line) and difference spectrum between spectra at 60 and 21 K; (b) $\mathbf{E}\parallel\mathbf{c}$ geometry at 21 K; derivative spectrum times -1 (dotted line) and difference spectrum between spectra at 35 and 21 K; different features are marked by A_1, A_2, A_3 in the $\mathbf{E}\parallel\mathbf{c}$ spectrum and B_0, B_1, B_2 in the $\mathbf{E}\parallel\mathbf{ab}$ spectrum. The corresponding positions of the maxima in the first derivative spectra are indicated by α_1, α_2 , and β_0 , and β_1 .

Absorption features in polarized XANES spectrum are due to full multiple scattering of the photoelectron emitted at the Cu site in the direction of the electric field of the x-ray beam and their physical origin has been previously discussed.³⁸ The features A_1 and A_2 are determined by multiple scattering of the ejected photoelectron off apical oxygen and La and Sr atoms and their temperature dependence preferentially probes structural changes perpendicular to the CuO_2 plane. The peak B_1 corresponds to multiple scattering of the photoelectron off oxygen and Cu atoms in the CuO_2 plane and its temperature dependence preferentially probes in-plane structural changes.

$\mathbf{E}\parallel\mathbf{ab}$ XANES spectra of the crystal in the HTT phase at 300 K are compared with spectra of the LTO phase at 100 and 150 K in Fig. 2. In addition to decrease in the intensities of the main peaks B_1 and B_2 , an increase in the intensity of the peak B_0 may be seen in the $\mathbf{E}\parallel\mathbf{ab}$ [panel (a)] case at the HTT \rightarrow LTO phase transition. There appears to be little change for the $\mathbf{E}\parallel\mathbf{c}$. Multiple scattering calculations of the Cu K -edge XANES spectrum³⁸ using atomic positions given by the average crystallographic structure do not predict such a large peak B_0 in the LTO phase. This peak was not observed in the $\mathbf{E}\parallel\mathbf{ab}$ XANES spectrum of undoped La_2CuO_4 (LCO) in the LTO structure.³⁹ The presence of this peak indicates that the local structure of the LTO phase of doped LSCO is

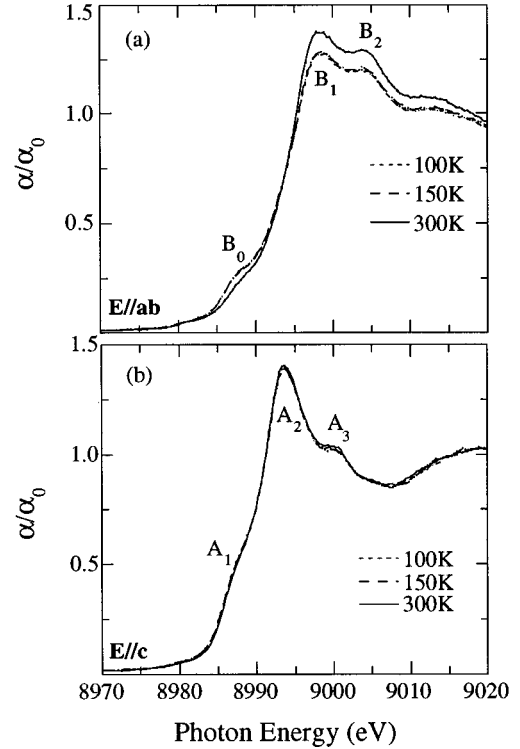


FIG. 2. XANES spectra across the HTT \rightarrow LTO transition: (a) $\mathbf{E}\parallel\mathbf{ab}$ spectrum in HTT phase at 300 K compared with spectra in the LTO phase at 100 and 150 K; (b) $\mathbf{E}\parallel\mathbf{c}$ spectrum in HTT phase at 300 K compared with spectra in the LTO phase at 100 and 150 K.

different from that of the LTO of undoped LCO. However, crystallographic techniques indicate that LCO at 300 K is structurally the same as LSCO in the LTO phase,⁴² and Cu K -edge EXAFS,⁴⁰ La K -edge EXAFS,⁵⁴ and neutron scattering experiments² probing the pair correlation function do not show any changes at the HTT \rightarrow LTO transition.

We have made absorption differences with respect to the spectrum measured at $T=21$ K to study the temperature dependence of different XANES features. The amplitudes of peaks in the difference spectra [see, e.g., spectra in panel (a) and (b) of Fig. 1] are well above the noise level. Statistical noise in the absorption coefficient of the normalized to the atomic absorption jump is less than $\pm 0.4\%$.

The temperature dependence of the XANES features of the LTO phase are shown in Fig. 3, where the absorption differences at the rising edges and at the absorption maxima are plotted. The intensities of the main peaks A_2 and B_1 are independent of temperature down to ~ 100 K and then increase monotonically down to the lowest temperature (21 K), A_2 by $\sim 5\%$ and B_1 by only $\sim 1.5\%$. Both B_1 and A_2 shift toward higher energy, indicated by the negative value of the absorption differences at the corresponding XANES derivative maxima β_1 and α_2 , which decrease by $\sim 5\%$. The energy shift reaches its maximum at ~ 35 K (the superconducting critical temperature T_c of the system) for α_2 and ~ 55 – 60 K ($\sim 1.6T_c$, hereafter called T^*) for β_1 . It is worth mentioning that Nohara *et al.*²⁵ have observed an anomalous change in the elastic constant of the LSCO system at around T^* . The far infrared (FIR) spectroscopic data have also shown an anomaly at ~ 60 K.⁵⁵

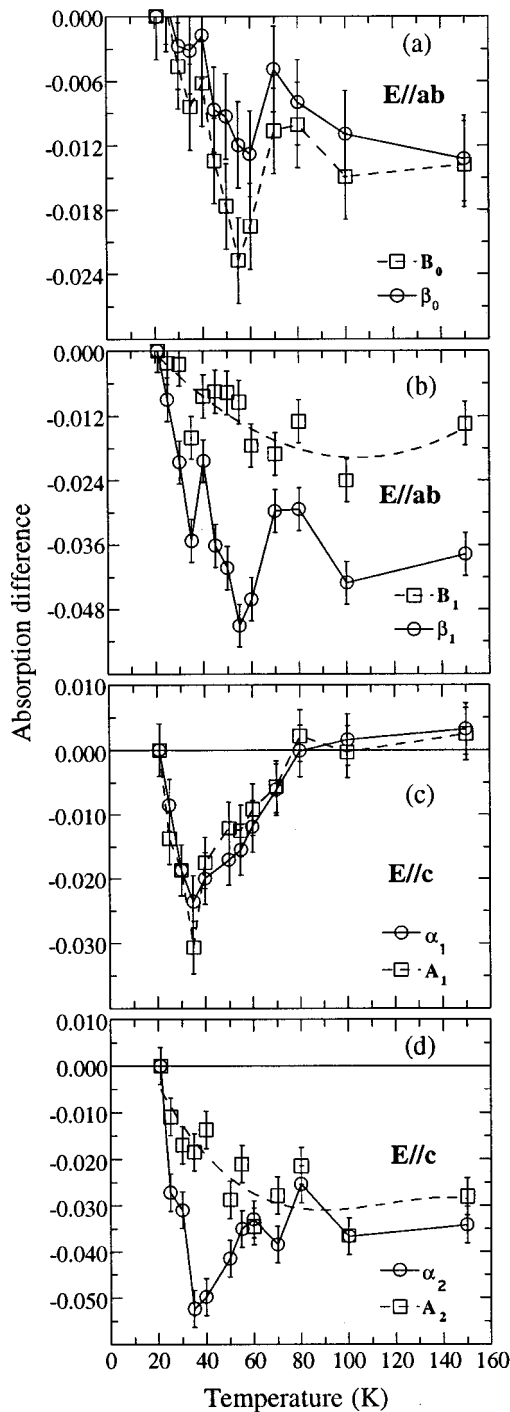


FIG. 3. Temperature dependence of amplitude of absorption differences at the energy positions of features β_0 , B_0 [panel (a)] and β_1 , B_1 [panel (b)] for $\mathbf{E}\parallel\mathbf{ab}$ XANES. Similarly, temperature dependence of features α_1 , A_1 and α_2 , A_2 for $\mathbf{E}\parallel\mathbf{c}$ XANES in panels (c) and (d). The estimated error ($\pm 0.4\%$) in the intensity differences is determined by experimental noise. Solid lines are a guide to the eye.

B. Local instability of the CuO_2 plane: EXAFS Fourier transform analysis

Figure 4 shows representative examples of the polarized Cu K -edge EXAFS signal (weighted by k^2) extracted from the measured absorption on the LSCO single crystal at 60 K

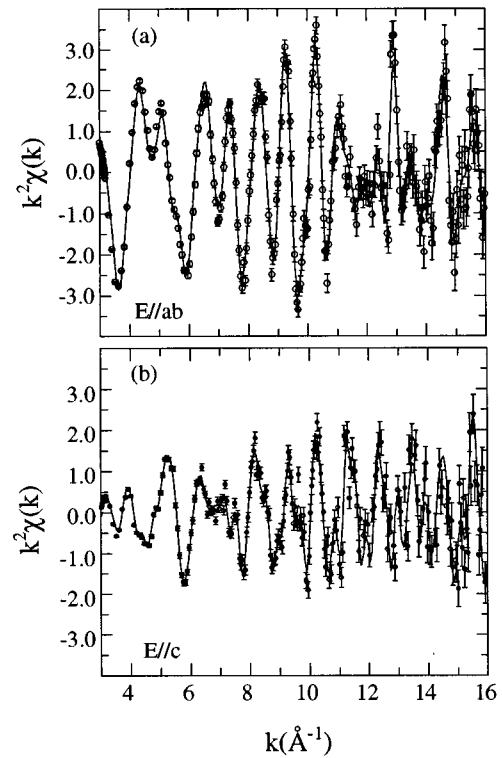


FIG. 4. Polarized Cu K -edge EXAFS signal multiplied by k^2 measured on single crystal $\text{La}_{1.85}\text{Sr}_{0.15}\text{CuO}_4$ at a representative temperature (60 K) in the (a) $\mathbf{E}\parallel\mathbf{ab}$ and (b) $\mathbf{E}\parallel\mathbf{c}$ geometries. Data points are shown with experimental noise. The solid line is a guide to the eye.

in the $\mathbf{E}\parallel\mathbf{ab}$ [panel (a)] and $\mathbf{E}\parallel\mathbf{c}$ [panel (b)] experimental geometries. The corresponding Fourier transforms $|\text{FT}(k^2\chi(k))|$ show that the signal of the Cu-O(planar) shell is completely suppressed in the $\mathbf{E}\parallel\mathbf{c}$ spectrum while the Cu-O(apical) signal is suppressed in the $\mathbf{E}\parallel\mathbf{ab}$ spectrum (not shown; see Ref. 43).

Figure 5 shows the temperature dependence of the Cu-O(planar) FT peak. The FT amplitude is plotted in panel (a) and amplitude of the EXAFS difference $[k^2(\chi(k) - \chi(21\text{ K}))]$ is shown in (b). [The FT of the $\mathbf{E}\parallel\mathbf{c}$ EXAFS has a double peaked structure at the Cu-O(apical) position⁴³ and did not show any systematic temperature dependence; this may be due to interference effects, and hence is not shown here.] At high temperature the FT signal is expected to be strongly dominated by thermal fluctuations of the atoms while it should increase due to decrease of the Debye-Waller factor at low temperatures.⁴⁰ The FT amplitude of the Cu-O(planar) peak decreases slightly or remains constant between 150 and 100 K. Below 100 K, this peak decreases greatly leaving an anomaly at ~ 60 K which corresponds to the characteristic temperature T^* .^{2,25,36,54} This anomaly in the FT of the $\mathbf{E}\parallel\mathbf{ab}$ EXAFS agrees well with the $\mathbf{E}\parallel\mathbf{ab}$ XANES anomaly discussed above.

It should be recalled that the variations of the EXAFS and XANES signals are quite large with a different temperature dependence and cannot be accounted by the expected variations of the Debye-Waller factors. A small increase (~ 0.001 Å) in the Cu-O(planar) distances below 170 K has been reported in crystallographic studies.²⁹ On the other hand, x-ray

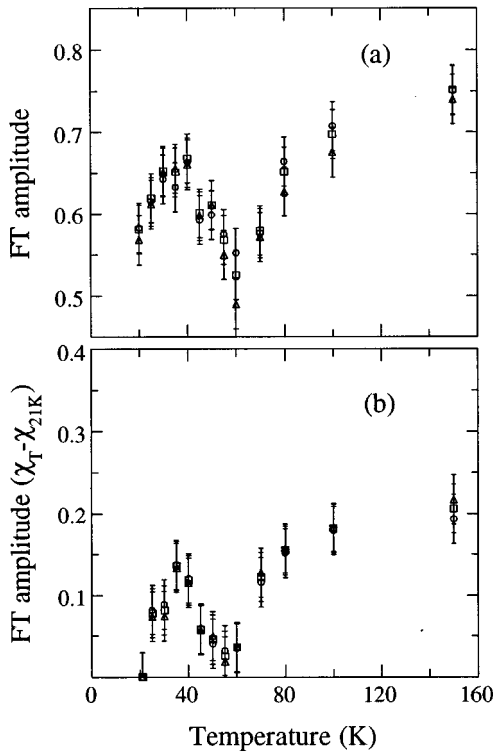


FIG. 5. Temperature dependence of the amplitude of the first shell, Cu-O(planar), peak in the Fourier transform. The temperature dependence of the amplitudes of the Fourier transform of the EXAFS difference, $|\text{FT}(k^2(\chi_T - \chi_{21\text{K}}))|$ at the positions of the FT peaks is shown in panel (b).

absorption spectroscopy (both EXAFS and XANES), which probe the short range order on a short time scale, show large variations and anomalies at two characteristic temperatures, T^* and T_c .

C. Determination of the local distortions and characterization of the minority distorted phase

The EXAFS signals of the Cu-O bonds in the two spectra are well separated from the longer bond contributions⁴³ and have been extracted by the standard Fourier filtering method. The filtered EXAFS signals represent single backscattering of the photoelectron emitted at the Cu site by its nearest neighbor oxygens and therefore probe the correlation function between Cu and oxygen pairs. Multiple scattering signals, which make the data analysis more complex, are not present because such contributions have a longer effective photoelectron pathlength. The first shell EXAFS due to Cu-O(planar) and Cu-O(apical) were fitted by nonlinear least squares fitting using curved wave EXAFS theory.⁴⁷

The results of the fit show two different distances below 100 K. These two distances converge to a single distance at $T > 100$ K, but the goodness of fit is 25% worse, indicating the possible presence even at higher temperatures of two distances that are not resolved in the present experiment. The temperature dependence of the two Cu-O(planar) distances (R_{short} and R_{long}) are shown in Fig. 6(a) and compared with the Cu-O(planar) distance measured by diffraction.^{29,42} The initial fit was performed using five parameters, R_{long} , R_{short} ,

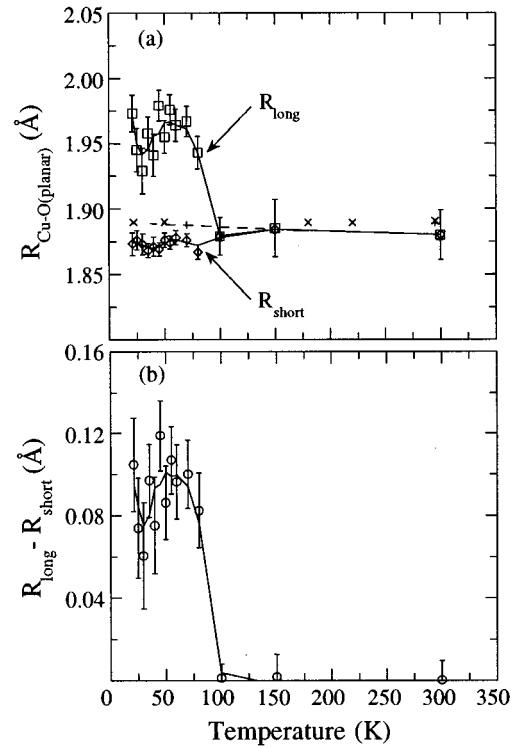


FIG. 6. (a) Temperature dependence of the two Cu-O(planar) distances (R_{short} and R_{long}) measured by EXAFS and the average distance measured by diffraction (cross from Ref. 29 and plus from Ref. 42); (b) temperature dependence of the difference between R_{short} and R_{long} .

N_{long} ($N_{\text{short}} = N_{\text{tot}} - N_{\text{long}}$, where N_{tot} is the fixed coordination number), and two Debye-Waller factors while the other parameters were fixed by fitting the EXAFS signal at room temperature of the present crystal and similar perovskites showing agreement with other reports.⁴⁹ The Debye-Waller factors are found to be similar and close to the values expected for the correlated Debye model and the values predicted by extrapolation of the Einstein model at low temperature. The final values of R_{long} , R_{short} , and $N_{\text{short}}/N_{\text{tot}}$ were obtained by the three parameters fit with Debye-Waller factors fixed to the correlated Debye model.

The average Cu-O(planar) distance obtained in the present EXAFS analysis agrees with diffraction^{29,42} and earlier EXAFS results.⁴⁰ It is worth mentioning that the Cu-O(planar) distances fall in the range of 1.87 to 1.97 Å roughly coinciding with the range of average Cu-O(planar) distances measured in different families of cuprate superconductors⁵⁶ (reproduced in Fig. 7). The separation between the two distances, shown in Fig. 6(b), varies between 0.06 and 0.12 Å, larger than the temperature fluctuations of the order of 0.02 Å for each distance.

The distortions in the CuO_4 square plane implied by the presence of two Cu-O(planar) distances appear to be correlated with the local tilting of the square plane in the $(0, \pi)$ direction as indicated by the anomalous behavior of the elastic constants.²⁵ We therefore ascribe the appearance of the anomalous long distance to tilting of the CuO_4 square plane as in the LTT structural domains, in which two oxygens per CuO_4 square plane are displaced along the c axis. The two types of Cu sites, with LTT and LTO tilts, are shown in Fig.

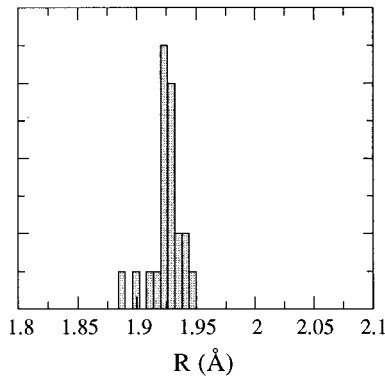


FIG. 7. Distribution of Cu-O(planar) distances determined by diffraction in 25 different cuprate superconductors, reported by Ihara *et al.* (Ref. 56).

8. The tilting angle θ of the CuO_4 square plane using $\cos \theta = R_{\text{short}}/R_{\text{long}}$, is in the range of 14° – 18° below 100 K. Similarly large tilt has been observed by NMR (Ref. 4) and neutron diffraction⁵⁷ in oxygen doped $\text{La}_2\text{CuO}_{4+\delta}$ and by neutron diffraction⁵⁸ and EXAFS (Refs. 11–14) in the Bi2212 system.

Below 100 K some $\sim 16\%$ of the Cu-O(planar) bonds are found to be anomalously long ($N_{\text{long}}/N_{\text{tot}}$). This implies that $33 \pm 3\%$ of the Cu sites have rhombic distortion (Fig. 8).

The filtered $\mathbf{E}||\mathbf{c}$ EXAFS spectra clearly show a beat (minima due to interference of two frequencies) at about 15 \AA^{-1} indicating the presence of different Cu-O(apical) distances. The temperature dependence of these two distances (R_{short} and R_{long}) and their separation (0.08 – 0.14 \AA) are shown in Fig. 9. This confirms earlier EXAFS studies⁴⁰ which reported an average Cu-O(apical) bond distance smaller (2.32 \AA) than that found in diffraction studies (2.4 \AA). R_{long} is close to the expected value for the average structure while R_{short} is clearly anomalous. Some 30% of the Cu-O(apical) bonds are short; this is similar to the proportion of rhombically distorted CuO_4 square planes. The short Cu-O(apical) distance is present even above 100 K and appears to be nearly temperature independent, in contrast to the anomalous long Cu-O(planar) distance (Fig. 6) which could not be identified at high temperature.

These in plane and out of plane bond length results show that the Cu local environment in the LSCO system is inho-

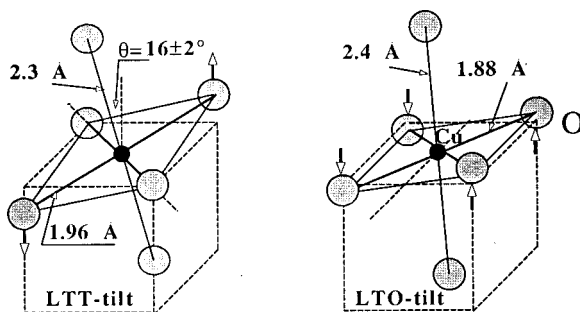


FIG. 8. Schematic of distorted CuO_6 octahedra with ‘‘LTT-type’’ tilt (left) and undistorted octahedra with ‘‘LTO-type’’ tilt (right).

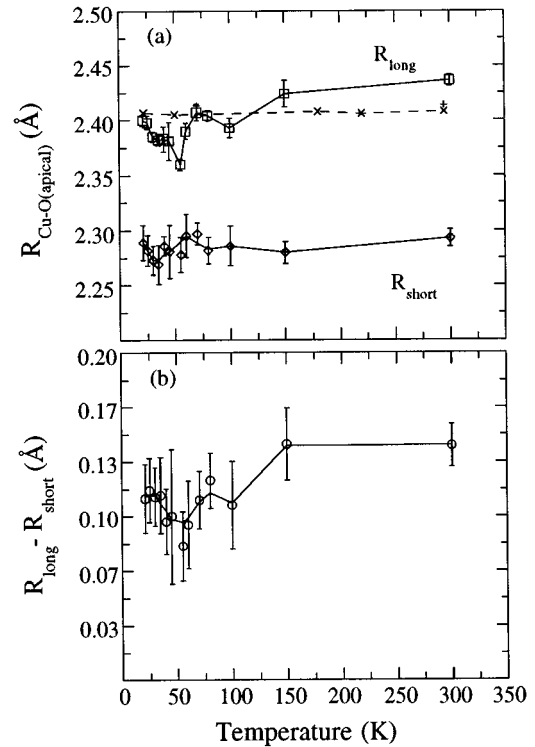


FIG. 9. (a) Temperature dependence of the two Cu-O(apical) distances (R_{short} and R_{long}) measured by EXAFS and the average distance measured by diffraction (cross from Ref. 29 and plus from Ref. 42); (b) temperature dependence of the difference between R_{short} and R_{long} .

mogeneous, containing about 33% rhombically distorted LTT (or $Pccn$) like domains. The results also confirm presence of both LTO and LTT structural domains below 60 K, previously indicated by splitting of a diffraction line.³⁶ Note that the local distortions we observe, involving elongation (contraction) of the in-plane (out of plane) bond lengths in the LTT-like Cu sites, are much larger than the differences between the bond lengths in the ‘‘average LTO’’ and ‘‘average LTT’’ crystallographic phases,¹⁶ because the highly distorted ‘‘local LTT-like sites’’ contribute only about 33% to the average phase.

D. Comparison with diffraction results: The Cu-O correlation from EXAFS and diffraction Debye-Waller factors and pair distribution function analysis

The Debye-Waller factor in the EXAFS measurements σ_{CuO}^2 is different from that observed in diffraction studies. The diffraction Debye-Waller factors correspond to the mean square deviation of copper (σ_{Cu}^2) and oxygen (σ_{O}^2) from their average crystallographic sites.^{29,42} On the other hand, EXAFS Debye-Waller factor σ_{CuO}^2 measures the correlated deviation in distance of the atomic pair consisting of the absorber (Cu) and backscatterer (O). The diffraction data show a single distance within the indetermination of atomic positions given by the Debye-Waller factors.^{29,42} Figure 10(a) shows the Debye-Waller factors measured by diffraction.

By using both the diffraction and EXAFS Debye-Waller factors, we can compute the degree of independence of mo-

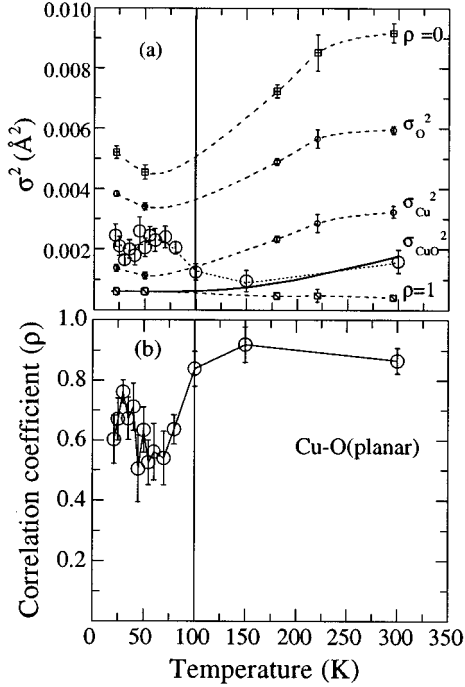


FIG. 10. (a) Temperature dependence of the EXAFS Debye-Waller factor σ_{CuO}^2 of the Cu-O(planar) distance extracted from the single shell fit of the **E||ab** EXAFS spectra (large open circles); and a fit with the Einstein model with Debye temperature $\theta_D=600$ K (solid line) for $T \geq 100$ K; diffraction Debye-Waller factors σ_{Cu}^2 and σ_{O}^2 for Cu and oxygen (open small circles from Ref. 29, and filled circles from Ref. 42); Debye-Waller factor σ_{CuO}^2 expected for correlated Cu-O motion ($\rho=1$), and uncorrelated motion ($\rho=0$). (b) Correlation coefficient ρ for instantaneous Cu-O distance measured by EXAFS.

tion of the Cu and O atoms. The correlation coefficient (ρ) of the Cu and O can be defined as $\text{COV}(\text{Cu},\text{O})/\sigma_{\text{Cu}}\sigma_{\text{O}}$ where $\text{COV}(\text{Cu},\text{O})$ is the covariance of the Cu and O and $\sigma_{\text{Cu}}(\sigma_{\text{O}})$ is the standard deviation from equilibrium of the Cu(O) site due to thermal vibrations, i.e., the diffraction Debye-Waller factor of Cu(O). We can calculate ρ from the relation $\rho = (\sigma_{\text{Cu}}^2 + \sigma_{\text{O}}^2 - \sigma_{\text{CuO}}^2)/2\sigma_{\text{Cu}}\sigma_{\text{O}} = \text{COV}(\text{Cu},\text{O})/\sigma_{\text{Cu}}\sigma_{\text{O}}$, where σ_{CuO}^2 is the EXAFS Debye-Waller factor. If $\rho=1$ the distance broadening between two neighboring atoms, measured by EXAFS, results from fully correlated instantaneous distribution of their atomic positions in space and time. If $\rho=0$ the distribution is fully uncorrelated. The Debye-Waller factor σ_{CuO}^2 expected for fully correlated Cu-O motion and uncorrelated motion are also shown (squares) in Fig. 10 (a).

We have measured the correlation coefficient at high temperature ($T \geq 100$ K) where a single Cu-O(planar) distance was observed. The correlation coefficient ρ was found to be ~ 0.9 showing correlated distribution of Cu and O at $T \geq 100$ K. We have extracted the effective correlation coefficient ρ at $T < 100$ K. For this purpose, the **E||ab** EXAFS signal was fitted imposing a single Cu-O(planar) distance as expected from the crystallographic data to obtain the Debye-Waller factor (σ_{CuO}^2). The fit was worse than what was obtained with two distances described in Sec. III B. The temperature dependence of the effective Debye-Waller factor is shown in Fig. 10(a). The onset of spatial inhomogeneity below 100 K

is reflected by the increase in the Debye-Waller factor. A similar increase of σ_{CuO}^2 was observed in $\text{La}_{1.875}\text{Ba}_{0.125}\text{CuO}_4$ (LBCO) at 1/8 doping below the LTO \rightarrow LTT transition temperature (60 K).⁵⁹ The solid line in Fig. 10(a) is the behavior of the Debye-Waller (DW) factor predicted by an Einstein model with Debye temperature $\theta_D=600$ K.

The effective correlation coefficient ρ at $T < 100$ K shows that the distribution is less correlated, with a minimum at T^* ($\rho \sim 0.5$). The temperature dependence of ρ is shown in Fig. 10(b). It is natural to think that the degree of freedom for distortions is lower in a correlated situation than in an uncorrelated one. Therefore at T^* the CuO_2 plane is expected to be comparatively distorted while at T_c distortions are reduced.

In Fig. 11 we show the Cu-O(planar) pair distribution function obtained by EXAFS at room temperature ($T=300$ K), in the normal phase in the range $T_s > T > T_c$ ($T=50$ K), at the transition temperature ($T_c=35$ K), and in the superconducting phase ($T=21$ K). It can be seen that at 50 and 21 K the two distances can be clearly distinguished while at 35 K the separation between the two is reduced producing merely an asymmetric Gaussian distribution. The pair correlation functions for the uncorrelated Cu-O pair ($\rho=0$) obtained from the Cu and O diffraction Debye-Waller factors^{29,42} are plotted for comparison. In no case is the observed splitting of the Cu-O distances at low temperature in disagreement with diffraction experiments, which were not able to resolve the two positions.

Figure 12(a) shows the pair distribution function of the Cu-O pairs in superconducting $\text{La}_{1.85}\text{Sr}_{0.15}\text{CuO}_4$ at 21 K compared with the pair distribution function of the Cu-O pairs in superconducting $\text{Bi}_2\text{Sr}_2\text{CaCu}_2\text{O}_{8+\delta}$ [panel (b)] as deduced from EXAFS at 30 K (Ref. 60) confirmed by anomalous x-ray diffraction.⁶¹ The distribution of Cu-O distances in $\text{La}_{1.85}\text{Sr}_{0.15}\text{CuO}_4$ is similar to the distribution of the average Cu-O distances in Bi2212 indicating similarity of the local structure of the CuO_2 plane in cuprate superconductors.

IV. DISCUSSION: THE STRIPE STRUCTURE OF THE CuO_2 PLANE

It has been proposed that an anharmonic one-dimensional (1D) modulation of the CuO_2 plane is a key feature to the mechanism of high- T_c superconductivity.^{14,62} An incommensurate superstructure of the type $\mathbf{q} = p\mathbf{b}^* + (1/n)\mathbf{c}^*$, in orthorhombic notation, has been observed in $\text{La}_{2-x}\text{Sr}_x\text{CuO}_4$ for $x \sim 0.075$ (Ref. 63) and $x=0.1$, and 0.15 (Ref. 64) by diffuse x-ray scattering. The superstructure peaks are much weaker in intensity for the overdoped sample $x=0.2$.⁶⁴ A similar 1D superstructure has been observed in oxygen doped $\text{La}_2\text{CuO}_{4+\delta}$.⁶⁵⁻⁶⁷

Joint analysis of EXAFS and diffraction data on Bi2212 system has permitted solution of local structure of the CuO_2 plane. It has been found that the distorted and undistorted CuO_2 planes are distributed spatially in two types of stripes.^{14,60} This approach to solving the stripe structure is based on the fact that a local probe (EXAFS) determines the statistical distribution of the local distortions while diffraction data provides the modulation period. In the case of a 1D modulation the statistical distribution is correlated with the character of the modulation; e.g., harmonic (anharmonic) character will produce a symmetric (asymmetric) distribu-

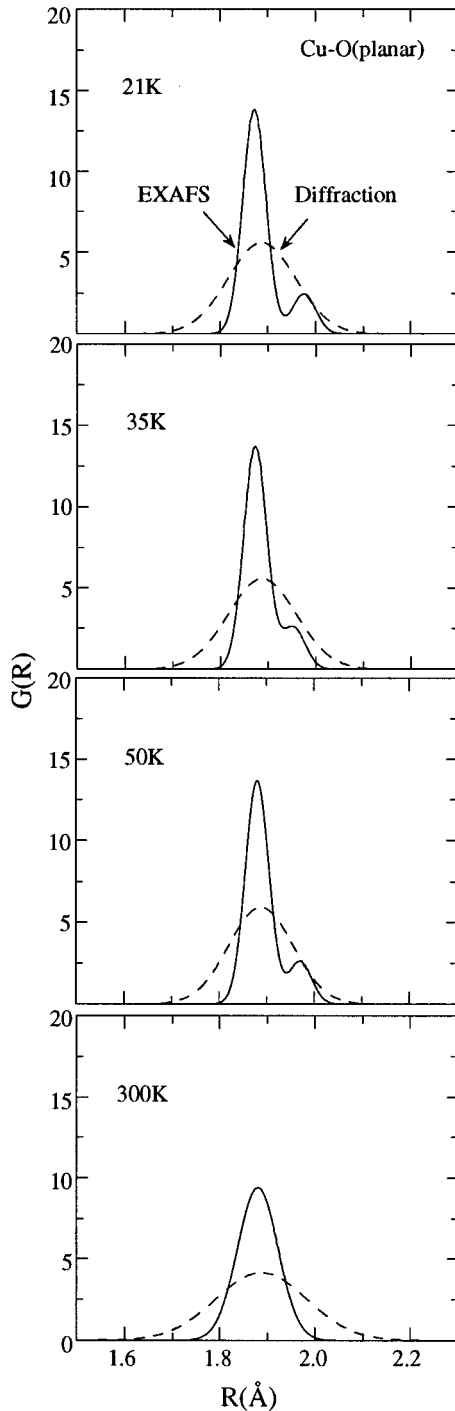


FIG. 11. Cu-O (planar) pair distribution in $\text{La}_{1.85}\text{Sr}_{0.15}\text{CuO}_4$ measured by EXAFS (solid lines) at $T=300$ K (RT); at $T=50$ K ($T_c < T < 100$ K), at $T=35$ K = T_c and in the superconducting phase at $T=21$ K. These are compared with the distribution of the Cu-O(planar) distances expected from diffraction data for the uncorrelated case ($\rho=0$) (dashed lines).

tion. Asymmetric distribution of the in-plane Cu-O bonds as shown in Figs. 11 and 12 demonstrates the anharmonic character of the modulation. In the case of largely anharmonic modulation the statistical distribution will not be a continuous but a two peak function. Therefore we interpret our PDF function as evidence of stripe structure of the CuO_2 plane, as in Bi2212 ,^{14,60} with the two types of Cu sites distributed

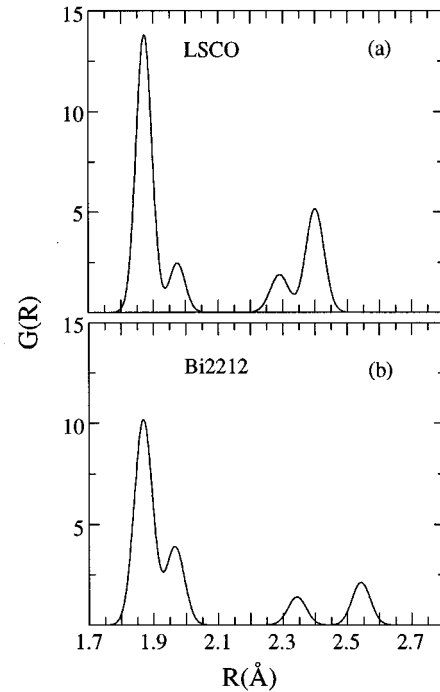


FIG. 12. Cu-O pair distribution in superconducting $\text{La}_{1.85}\text{Sr}_{0.15}\text{CuO}_4$ at 21 K [panel (a)] compared with the Cu-O pair distribution in superconducting $\text{Bi}_2\text{Sr}_2\text{CaCu}_2\text{O}_{8+\delta}$ at 30 K [panel (b)].

spatially. The undistorted (U) stripes with Cu sites of the LTO type are alternated by distorted (D) stripes with Cu sites of the LTT or $Pccn$ type.

The modulation period measured by diffraction is $\lambda_p = L + W \approx 24$ Å, where W is the width of the D stripes and L the width of the U stripes. The ratio W/λ_p is essentially the proportion of distorted Cu sites measured by EXAFS which is $\approx 33\%$. The width W of the LTT-like stripes is then $W \sim 24 \times 0.33 \sim 8$ Å and the width of LTO-like stripes $L \sim 16$ Å, below 100 K. Statt *et al.*⁶⁸ followed a similar approach to study stripe structure in oxygen doped $\text{La}_2\text{CuO}_{4+\delta}$. They used joint analysis of NMR data to probe the octahedral tilt distribution and diffraction data to provide the modulation period. 1D modulation of the superconducting gap observed using scanning tunneling microscopy has shown a stripe structure in YBCO.⁶⁹

Inelastic neutron scattering studies⁷⁰⁻⁷³ on the LSCO system have shown well resolved dynamic magnetic incommensurate fluctuations below 100 K. These magnetic incommensurate peaks have been first assigned to dynamical fluctuation related with nesting vectors of the Fermi surface; however, it is possible that they are due to one-dimensional ordering of magnetic domains with linear domain walls.

The temperature onset for the freezing of two different Cu site conformations observed here appear to occur in the same temperature range where dynamic magnetic incommensurate fluctuations are well resolved. This result suggests that the two effects are correlated. It is interesting to note that in the superconducting phase of LSCO, the incommensurate magnetic superstructure in the inelastic neutron scattering⁷⁰⁻⁷³ appears at 45° from the stripe direction determined by elastic x-ray diffraction.⁶³ This is not the case in the insulating

doped nickelates $\text{La}_{2-x}\text{Sr}_x\text{NiO}_4$ where both magnetic and structural modulation follow the same direction.^{63,74}

V. CONCLUSIONS

The large tilt and the elongation of the in-plane Cu-O distances in the D stripes indicates that the electronic structure in the D stripes is different from that in the U stripes.¹⁷ The electron lattice instability driving the 2D lattice towards the formation of alternate LTT and LTO stripes of different electronic structure was first observed in Bi2212 and assigned to ordering of pseudo-Jahn-Teller ($3d_z^2$) polarons in a 1D charge density wave (CDW).⁷⁵ Lattice instability due to a dynamic Jahn-Teller effect has been shown to drive the CuO_2 lattice to form alternate LTO and LTT stripes.⁷⁶ The measured tilt in the distorted Cu sites is larger than the critical tilt for charge localization as determined by Büchner *et al.*¹⁷ In fact the large LTT-like tilt introduces splitting of the bands around the M point of the Fermi surface and opens a partial gap in the density of states at the van Hove peak. This pseudogap opens quadratically with distortion from the HTT phase, and the expected drop of the density of states (DOS) at the Fermi level is sufficient to account for the loss of superconductivity in the LTT-like stripes.^{77,78}

Our experimental results support a “two component” pairing model in which a free electron gas confined in a superlattice of quantum U stripes is coupled with a second electronic component, a Wigner CDW confined in parallel D stripes.^{13,79} This model is different from several proposed pairing mechanisms involving two electronic components in a homogeneous lattice.^{80–83}

By comparing the stripe structure in the superconducting phase of $\text{La}_{2-x}\text{Sr}_x\text{CuO}_4$ with that in insulating systems, as in

doped nickelates⁶³ and cuprates at anomalous 1/8 doping,⁸⁴ we can see that in the latter case all doped charges are frozen in a short wavelength (about 4 Cu sites) 1D CDW while in the superconducting phase only a small portion of charges is frozen in a long wavelength (about nine Cu sites) 1D CDW. This CDW is not a standard CDW due to the instability of the Fermi surface to lattice distortions, but it could be assigned to charge ordering driven by Coulomb interactions and can be called generalized Wigner CDW.⁷⁹

LSCO, with $T_c = 35$ K, is a member of the high- T_c cuprate perovskites with critical temperatures in the range 23–150 K, while in conventional superconductors the critical temperature is ≤ 23 K. The enhancement of T_c by a factor 10–100 has been attributed to a resonance effect in the pairing mechanism, in which a superconducting electron gas in a superlattice of quantum stripes of width L is tuned to a “shape resonance” condition $L \sim n\lambda_F/2$ (with λ_F the wavelength of the electrons at the Fermi level and n an integer) by changes in the charge density and/or the stripe width L .¹⁴

The stripe width L has been determined to be 15 ± 0.5 Å and 16 Å in the Bi2212 (Ref. 14) and LSCO, respectively. We find, using a BCS approach, that a superlattice of quantum stripes having L in the range 14–16 Å increases the superconducting gap by a factor of 6–100 over a homogeneous lattice at optimum doping.⁸⁵

ACKNOWLEDGMENTS

We acknowledge experimental help from Dr. M. Missori and T. Rossetti. We would like to thank the Istituto Nazionale di Fisica Nucleare (INFN), Istituto Nazionale di Fisica della Materia (INFM), and Consiglio Nazionale delle Ricerche (CNR) for financial assistance.

¹For a review see, e.g., T. Egami, and S. J. L. Billinge, *Prog. Mater. Sci.* **38**, 359 (1994).

²B. H. Toby, T. Egami, J. D. Jorgensen, and M. A. Subramanian, *Phys. Rev. Lett.* **64**, 2414 (1990); S. J. L. Billinge, T. Egami, D. R. Richards, D. G. Hinks, D. Dabrowski, J. D. Jorgensen, and K. Violin, *Physica C* **179**, 279 (1991); S. J. L. Billinge and T. Egami, *Phys. Rev. B* **47**, 14 386 (1993).

³J. Mustre de Leon, S. D. Conradson, I. Batistic, and A. R. Bishop, *Phys. Rev. Lett.* **65**, 1675 (1990); S. D. Conradson, I. D. Raistrick, and A. R. Bishop, *Science* **248**, 1394 (1990); J. Mustre de Leon, I. Batistic, A. R. Bishop, S. D. Conradson, and S. A. Trugman, *Phys. Rev. Lett.* **68**, 3236 (1992); J. Mustre de Leon, S. D. Conradson, I. Batistic, A. R. Bishop, I. D. Raistrick, M. C. Aronson, and F. H. Garzon, *Phys. Rev. B* **45**, 2447 (1992); J. Mustre de Leon, S. D. Conradson, I. Batistic, A. R. Bishop, I. D. Raistrick, M. C. Aronson, and F. H. Garzon, *ibid.* **47**, 12 322 (1993).

⁴P. C. Hammel, A. P. Reyes, S.-W. Cheong, and Z. Fisk, *Phys. Rev. Lett.* **71**, 440 (1993); P. C. Hammel, in *Phase Separation in Cuprate Superconductors*, edited by E. Sigmund and A. K. Müller (Springer-Verlag, Berlin-Heidelberg, 1994).

⁵M. A. Teplov, O. N. Bakharev, A. V. Dooglav, A. V. Egorov, E. V. Krjukov, O. Marvin, V. V. Naletov, A. G. Volodin, and D. Wagener, *Physica C* **235-240**, 265 (1994).

⁶*Lattice Effects in High- T_c Superconductors*, Proceedings of the meeting, Santa Fe, New Mexico, 1992, edited by Y. Bar-Yam, T. Egami, J. Mustre de Leon, and A. R. Bishop (World Scientific, Singapore, 1992).

⁷*Phase Separation in Cuprate Superconductors*, Proceedings of the meeting, Erice, Italy, 1992, edited by K. A. Müller and G. Benedek (World Scientific, Singapore, 1993).

⁸*Phase Separation in Cuprate Superconductors*, Proceedings of the Workshop, Cottbus, Germany, 1993, edited by E. Sigmund and A. K. Müller (Springer-Verlag, Berlin-Heidelberg, 1994).

⁹J. Röhler, A. Larisch, and R. Schafer, *Physica C* **191**, 57 (1991); J. Röhler, in *Materials and Crystallographic Aspects of HTc-Superconductivity*, edited by E. Kaldis (Kluwer Academic, Netherlands, 1994), p. 353.

¹⁰H. Oyanagi, *Bull. Electrotech. Lab.* **58**, 29 (1994); H. Yamaguchi, S. Nakajima, Y. Kuwahara, H. Oyanagi, and Y. Syono, *Physica C* **213**, 375 (1993), and references cited therein.

¹¹A. Bianconi, S. Della Longa, M. Missori, I. Pettiti, and M. Pompa, in *Lattice Effects in High- T_c Superconductors*, edited by Y. Bar-Yam, T. Egami, J. Mustre de Leon, and A. R. Bishop (World Scientific, Singapore, 1992), p. 65.

¹²A. Bianconi, S. Della Longa, M. Missori, I. Pettiti, M. Pompa, and A. Soldatov, *Jpn. J. Appl. Phys.* **32** (Suppl. 32-2), 578 (1993).

- ¹³A. Bianconi, M. Missori, H. Oyanagi, H. Yamaguchi, D. H. Ha, and Y. Nishihara, *Bull. Electrotech. Lab.* **58**, 16 (1994); A. Bianconi and M. Missori, in *2nd Workshop on "Phase Separation in Cuprate Superconductors,"* Cottbus, Germany, 1993, edited by E. Sigmund and A. K. Müller (Springer-Verlag, Berlin-Heidelberg, 1994), p. 272.
- ¹⁴A. Bianconi and M. Missori, *J. Phys. I (France)* **4**, 361 (1994); M. Missori, A. Bianconi, H. Oyanagi, and H. Yamaguchi, *Physica C* **235-240**, 1245 (1994); A. Bianconi, M. Missori, H. Oyanagi, H. Yamaguchi, D. H. Ha, Y. Nishiara, and S. Della Longa, *Europhys. Lett.* **31**, 411 (1995).
- ¹⁵S. J. L. Billinge, G. H. Kwei, and H. Takagi, *Phys. Rev. Lett.* **72**, 2282 (1994).
- ¹⁶J. D. Axe and M. K. Crawford, *J. Low Temp. Phys.* **95**, 271 (1994).
- ¹⁷B. Büchner, M. Breuer, A. Freimuth, and A. P. Kampf, *Phys. Rev. Lett.* **73**, 1841 (1994).
- ¹⁸Y. N. Wang, J. Wu, J. Zhu, H. Shem, J. Zhang, Y. Yan, and Z. Zhao, *Physica C* **162-164**, 454 (1989); X. H. Chen, Y.-N. Wang, and H. M. Shen, *Mod. Phys. Lett. B* **3**, 1241 (1989); Y.-N. Wang, H. M. Shen, M. Zhu, and J. Wu, *Solid State Commun.* **76**, 1273 (1990); S. L. Yuan, W. Y. Guan, Z. J. Chen, Y. L. Yuan, Y. B. Jia, J. Q. Zheng, B. Zhu, W. Wang, and G. G. Zheng, *Mod. Phys. Lett. B* **3**, 685 (1989); Y.-N. Wang, in *Proceedings of the Beijing International Conference on High-Temperature Superconductivity (BHTSC'92)*, edited by Z. Z. Gan, S. S. Xie, and Z. X. Zhao (World Scientific, Singapore, 1993), p. 147.
- ¹⁹M. Saint-Paul, J. L. Tholence, H. Noël, J. C. Levet, M. Potel, and P. Gougeon, *Physica C* **166**, 404 (1990).
- ²⁰H. A. Mook, M. Mostoller, J. A. Harvey, N. W. Hill, B. C. Chakoumakos, and B. C. Sales, *Phys. Rev. Lett.* **65**, 2869 (1990).
- ²¹H. A. Mook, B. C. Chakoumakos, M. Mostoller, A. T. Boothroyd, and Mc K. Paul, *Phys. Rev. Lett.* **69**, 2272 (1992).
- ²²T. Haga, K. Yamaya, Y. Abe, Y. Tajima, and Y. Hidaka, *Phys. Rev. B* **41**, 826 (1990).
- ²³K. Yamaya, T. Haga, and Y. Abe, *Bull. Electrotech. Lab.* **58**, 25 (1994).
- ²⁴K. Yamaya, in *Lattice Effects in High- T_c Superconductors*, Proceedings of the meeting, Santa Fe, New Mexico, 1992, edited by Y. Bar-Yam, T. Egami, J. Mustre de Leon, and A. R. Bishop (World Scientific, Singapore, 1992).
- ²⁵M. Nohara, T. Suzuki, Y. Maeno, T. Fijita, I. Tanaka, and H. Kojima, *Phys. Rev. Lett.* **70**, 3447 (1993); *Phys. Rev. B* **52**, 570 (1995).
- ²⁶A. Migliori, T. Chen, B. Alavi, and G. Gruner, *Solid State Commun.* **63**, 827 (1987); *Phys. Rev. B* **41**, 2098 (1990).
- ²⁷T. Fukase, T. Nomoto, T. Hanaguri, T. Goto, and Y. Koiche, *Physica B (Amsterdam)* **165&166**, 1289 (1990).
- ²⁸M. Lang, R. Kürsch, A. Grauel, C. Geibel, F. Steglich, H. Rietschel, T. Wolf, Y. Hidaka, K. Kumagai, Y. Maeno, and T. Fujita, *Phys. Rev. Lett.* **69**, 482 (1992).
- ²⁹M. Braden, P. Schweiss, G. Heger, W. Reichardt, Z. Fisk, K. Gamayunov, I. Tanaka, and H. Kojima, *Physica C* **223**, 396 (1994).
- ³⁰M. Braden, O. Hoffels, W. Schnelle, B. Büchner, G. Heger, B. Hennion, I. Tanaka, and H. Kojima, *Phys. Rev. B* **47**, 12 288 (1993).
- ³¹M. Arai, K. Yamada, Y. Hidaka, S. Itoh, Z. A. Bowden, A. D. Taylor, and Y. Endoh, *Phys. Rev. Lett.* **69**, 359 (1992).
- ³²M. Arai, K. Yamada, Y. Hidaka, A. D. Taylor, and Y. Endoh, *Physica C* **181**, 45 (1991); M. Arai, K. Yamada, S. Hosoya, A. C. Hannon, Y. Hidaka, A. D. Taylor, and Y. Endoh, *Bull. Electrotech. Lab.* **58**, 22 (1994).
- ³³S. Battacharya, M. J. Higgings, D. C. Johnston, A. J. Jacobson, J. P. Stokes, D. Goshorn, and J. T. Lewandowski, *Phys. Rev. Lett.* **60**, 1181 (1988).
- ³⁴J. B. Goodenough and A. Manthiram, *Solid State Chem.* **88**, 115 (1990); J. B. Goodenough, J.-S. Zhou, and K. Allan, *J. Mater. Chem.* **1**, 715 (1991).
- ³⁵Y. N. Wang, H. M. Shen, and J. S. Zhu, *J. Phys. C* **20**, L665 (1987).
- ³⁶Z. J. Yang, M. Yewondwossen, R. A. Dunlap, D. J. W. Geldart, S. L. Yuan, T. Kimura, K. Kishio, and K. Kitazawa, *Phys. Lett. A* **197**, 439 (1995).
- ³⁷*X-Ray Absorption: Principle, Applications Techniques of EXAFS, SEXAFS and XANES*, edited by R. Prinz and D. Koningsberger (Wiley, New York, 1988).
- ³⁸C. Li, M. Pompa, A. Congiu Castellano, S. Della Longa, and A. Bianconi, *Physica C* **175**, 369 (1991).
- ³⁹H. Oyanagi, K. Oka, H. Unoki, Y. Nishihara, K. Murata, H. Yamaguchi, T. Matsushita, M. Tokumoto, and Y. Kimura, *J. Phys. Soc. Jpn.* **58**, 2896 (1989).
- ⁴⁰J. B. Boyce, F. Bridges, T. Claeson, T. H. Geballe, C. W. Chu, and J. M. Tarascon, *Phys. Rev. B* **35**, 7203 (1987); *Phys. Scr.* **37**, 912 (1988); J. M. Tranquada, S. M. Heald, A. R. Moodenbaugh, and M. Suenaga, *Phys. Rev. B* **35**, 7187 (1987).
- ⁴¹H. Takagi, T. Ido, S. Ishibashi, M. Uota, S. Uchida, and Y. Tokura, *Phys. Rev. B* **40**, 2254 (1989); H. Takagi, R. J. Cava, M. Marezio, B. Batlogg, J. J. Krajewski, W. F. Peck, Jr., P. Bordet, and D. E. Cox, *Phys. Rev. Lett.* **69**, 2975 (1992).
- ⁴²P. G. Radaelli, D. G. Hinks, A. W. Mitchell, B. A. Hunter, J. L. Wagner, B. Dabrowsky, K. G. Vandervoort, H. K. Viswanathan, and J. D. Jorgensen, *Phys. Rev. B* **49**, 4163 (1994).
- ⁴³A. Bianconi, N. L. Saini, A. Lanzara, M. Missori, T. Rossetti, H. Oyanagi, H. Yamaguchi, K. Oka, and T. Ito, *Phys. Rev. Lett.* **76**, 3412 (1996).
- ⁴⁴J. C. Mikkelsen, Jr. and J. B. Boyce, *Phys. Rev. B* **28**, 7130 (1983); N. Motta, A. Balzarotti, P. Letardi, M. Podgorny, M. T. Czyzyk, A. Kisiel, and M. Zimnal-Starnawska, *Solid State Commun.* **53**, 509 (1985).
- ⁴⁵H. Oyanagi, T. Matsushita, H. Tanoue, T. Ishiguro, and K. Kohra, *Jpn. J. Appl. Phys.* **24**, 610 (1985).
- ⁴⁶L. Tröger, D. Arvanitis, K. Baberschke, H. Michaelis, U. Grimm, and E. Zschech, *Phys. Rev. B* **46**, 3283 (1992); J. Goulon, C. Goulon-Ginet, R. Cortes, and J. M. Dubois, *J. Phys. I (France)* **43**, 539 (1982).
- ⁴⁷S. J. Gurman, N. Binsted, and I. Ross, *J. Phys. C* **17**, 143 (1984); **19**, 1845 (1986).
- ⁴⁸J. J. Rehr, J. Mustre de Leon, S. I. Zabinsky, and R. C. Albers, *J. Am. Chem. Soc.* **113**, 5135 (1991); J. Mustre de Leon, J. J. Rehr, S. I. Zabinsky, and R. C. Albers, *Phys. Rev. B* **44**, 4146 (1991).
- ⁴⁹G. G. Li, F. Bridges, and C. H. Booth, *Phys. Rev. B* **52**, 6332 (1995).
- ⁵⁰Report of the International Workshop on Standards and Criteria in X-ray Absorption Spectroscopy, edited by F. W. Lytle, D. E. Sayers, and E. A. Stern [*Physica B* **158**, 701 (1989)]; *XAFS in X-ray Absorption Fine Structure*, edited by S. Hasnain (Ellis Horwood, England, 1991), p. 751.
- ⁵¹R. W. Joyner, K. J. Martin, and P. Meehan, *J. Phys. C* **20**, 4005 (1987).

- ⁵²M. Sánchez del Rìo (unpublished); S. Mobilio, F. Comin, and L. Incoccia (unpublished).
- ⁵³A. Kuzmin and J. Purans, *J. Phys. Condens. Matter* **5**, 267 (1993); **5**, 2333 (1993); **5**, 9423 (1993).
- ⁵⁴D. Haskel, E. A. Stern, D. G. Hinks, A. W. Michell, J. D. Jorgensen, and J. I. Budnick, *Phys. Rev. Lett.* **76**, 439 (1996).
- ⁵⁵Y. Yagil and E. Salje, *Physica C* **229**, 152 (1994).
- ⁵⁶H. Ihara, *Bull. Electrotech. Lab.* **58**, 64 (1994); also see, e.g., F. Izumi and E. Takayama-Muromachi, in *High Temperature Superconducting Materials and Engineering*, edited by D. Shi (Pergamon, New York, 1995), p. 81.
- ⁵⁷P. G. Radaelli, J. D. Jorgensen, A. J. Shultz, B. A. Hunter, J. L. Wagner, F. C. Chou, and D. C. Johnston, *Phys. Rev. B* **48**, 499 (1993).
- ⁵⁸A. Yamamoto, M. Onoda, E. Takayama-Muromachi, F. Izumi, T. Ishigaki, and H. Asano, *Phys. Rev. B* **42**, 4228 (1990); A. I. Beskrovnyi, M. Dlouhá, Z. Jirák, S. Vratislav, and E. Pollert, *Physica C* **166**, 79 (1990); A. I. Beskrovnyi, M. Dlouhá, Z. Jirák, and S. Vratislav, *ibid.* **171**, 19 (1990).
- ⁵⁹A. Lanzara, N. L. Saini, T. Rossetti, A. Bianconi, H. Oyanagi, H. Yamaguchi, and Y. Maeno, *Solid State Commun.* **97**, 93 (1996).
- ⁶⁰N. L. Saini, T. Rossetti, A. Lanzara, M. Missori, A. Perali, H. Oyanagi, and A. Bianconi, *J. Supercond.* **9**, 343 (1996); A. Bianconi, N. L. Saini, T. Rossetti, A. Lanzara, A. Perali, M. Missori, H. Oyanagi, H. Yamaguchi, Y. Nishihara, and D. H. Ha, *Phys. Rev. B* **54**, 12018 (1996).
- ⁶¹A. Bianconi, M. Lusignoli, N. L. Saini, P. Bordet, Å. Kvik, and P. G. Radaelli, *Phys. Rev. B* **54**, 4310 (1996).
- ⁶²A. Bianconi, *Solid State Commun.* **89**, 933 (1994); A. Bianconi, M. Missori, N. L. Saini, H. Oyanagi, H. Yamaguchi, D. H. Ha, and Y. Nishiara, *J. Supercond.* **8**, 545 (1995).
- ⁶³E. D. Isaacs, G. Aeppli, P. Zschack, S.-W. Cheong, H. Williams, and D. J. Buttrey, *Phys. Rev. Lett.* **72**, 3421 (1994); E. D. Isaacs, G. Aeppli, S.-W. Cheong, and P. Zschack (unpublished).
- ⁶⁴W. Dmowski, R. J. McQueeney, T. Egami, Y. P. Feng, S. K. Sinha, T. Hinatsu, and S. Uchida, *Phys. Rev. B* **52**, 6829 (1995).
- ⁶⁵N. Lagueyte, F. Weill, A. Wattiaux, and J.-C. Grenier, *Eur. J. Solid State Inorg. Chem.* **30**, 859 (1993).
- ⁶⁶P. G. Radaelli, J. D. Jorgensen, A. J. Shultz, B. A. Hunter, J. L. Wagner, F. C. Chou, and D. C. Johnston, *Phys. Rev. B* **48**, 499 (1993).
- ⁶⁷X. Xiong, P. Wochner, S. C. Moss, Y. Cao, K. Koga, and N. Fujita, *Phys. Rev. Lett.* **76**, 2997 (1996).
- ⁶⁸B. W. Statt, P. C. Hammel, Z. Fisk, S.-W. Cheong, F. C. Chou, D. C. Johnston, and J. E. Schirber, *Phys. Rev. B* **52**, 15 575 (1995).
- ⁶⁹H. L. Edwards, D. J. Derro, A. L. Barr, J. T. Market, and A. L. de Lozanne, *Phys. Rev. Lett.* **75**, 1387 (1995).
- ⁷⁰H. Yoshizawa, S. Mitsuda, H. Kitazawa, and K. Katsumada, *J. Phys. Soc. Jpn.* **57**, 3686 (1988).
- ⁷¹T. E. Mason, G. Aeppli, and H. A. Mook, *Phys. Rev. Lett.* **68**, 1414 (1992).
- ⁷²M. Matsuda, K. Yamada, Y. Endoh, T. R. Thurston, G. Shirane, R. J. Birgeneau, M. K. Kastner, I. Tanaka, and H. Kojima, *Phys. Rev. B* **49**, 6958 (1994).
- ⁷³T. R. Thurston, P. M. Gehring, G. Shirane, R. J. Birgeneau, M. K. Kastner, Y. Endoh, M. Matsuda, K. Yamada, H. Kojima, and I. Tanaka, *Phys. Rev. B* **46**, 9128 (1992).
- ⁷⁴S. M. Hayden, G. H. Lander, J. Zarestky, P. J. Brown, C. Stassis, P. Metcalf, and J. M. Honing, *Phys. Rev. Lett.* **68**, 1061 (1992).
- ⁷⁵A. Bianconi, in *International Conference on Superconductivity*, Bangalore, 1990, edited by S. K. Joshi, C.N.R. Rao, and S. V. Subramanyam (World Scientific, Singapore, 1990), p. 448.
- ⁷⁶R. S. Markiewicz, *Physica C* **200**, 65 (1992); **217**, 381 (1993); **210**, 235 (1993); **210**, 264 (1993); **207**, 281 (1993).
- ⁷⁷J. Fridel, *J. Phys. Condens. Matter* **1**, 7757 (1989).
- ⁷⁸W. E. Pickett, R. E. Cohen, and K. Krakauer, *Phys. Rev. Lett.* **67**, 228 (1991); R. E. Cohen, W. E. Pickett, D. Papaconstantopoulos, and H. Krakauer, in *Lattice Effects in High- T_c Superconductors*, edited by Y. Bar-Yam *et al.* (World Scientific, Singapore, 1992), p. 223.
- ⁷⁹A. Bianconi, *Solid State Commun.* **91**, 1 (1994); A. Bianconi and M. Missori, *ibid.* **91**, 287 (1994).
- ⁸⁰R. Fridberg and T. D. Lee, *Phys. Rev. B* **40**, 6745 (1989).
- ⁸¹Y. Bar Yam, *Phys. Rev. B* **43**, 2601 (1991).
- ⁸²J. Ranninger, J. M. Robin, and M. Eschrig, *Phys. Rev. Lett.* **74**, 4027 (1995).
- ⁸³J. Ashkenazi, *J. Supercond.* **8**, 559 (1995).
- ⁸⁴J. M. Tranquada, B. J. Sternlieb, J. D. Axe, Y. Nakamura, and S. Uchida, *Nature* **375**, 561 (1995).
- ⁸⁵A. Perali, A. Bianconi, A. Lanzara, and N. L. Saini, *Solid State Commun.* **100**, 181 (1996).